



Development of a sensitive and quantitative capillary LC-UV method to study the uptake of pharmaceuticals in zebrafish brain

Stanislav Kislyuk¹ · Wannes Van den Bosch¹ · Erwin Adams¹ · Peter de Witte² · Deirdre Cabooter¹ 

Received: 2 December 2017 / Revised: 5 February 2018 / Accepted: 8 February 2018 / Published online: 27 February 2018
© Springer-Verlag GmbH Germany, part of Springer Nature 2018

Abstract

The present study explores the potential of 10-day-old zebrafish (*Danio rerio*) as a predictive blood-brain-barrier model using a set of 7 pharmaceutical agents. For this purpose, zebrafish were incubated with each of these 7 drugs separately via the route of immersion and the concentration reaching the brain was determined by applying a brain extraction procedure allowing isolation of the intact brain from the head of the zebrafish larvae. Sample analysis was performed utilizing capillary ultra-high performance liquid chromatography (cap-UHPLC) on a Pepmap RSLC C18 capillary column (150 mm × 300 μm, $d_p = 2 \mu\text{m}$) coupled to a variable wavelength UV detector. Gradient separation was performed in 28 min at a flow rate of 5 μL/min and the optimal injection volume was determined to be 1 μL. The brain extraction procedure was established for the zebrafish strain TG898 exhibiting red fluorescence of the brain, allowing control of the integrity of the extracted parts. Quantitative experiments carried out on pooled samples of six zebrafish ($n = 6$) demonstrated the selective semipermeable nature of the blood-brain barrier after incubating the zebrafish at the maximum tolerated concentration for the investigated pharmaceuticals. The obtained brain-to-trunk ratios ranged between 0.3 for the most excluded compound and 1.2 for the pharmaceutical agent being most accumulated in the brain of the fish.

Keywords Zebrafish · Blood-brain barrier · Capillary UHPLC · Method development · Sample preparation

Introduction

The blood-brain barrier (BBB) does not only protect the human brain against chemical or biological intruders but also maintains stable conditions in the abluminal environment. As the main function of the BBB is the support of homeostasis in the brain, only molecules with certain qualities can pass it [1]. Since the BBB can prevent effective drug distribution into

the brain, problems of successful target attainment are one of the major concerns during the development of novel drugs addressing the central nervous system (CNS). This is underlined by the fact that more than 98% of newly discovered CNS drugs are incapable of penetrating the BBB [2]. Due to the selective nature of the BBB, one of the major challenges of treating CNS diseases is to achieve a safe and efficacious drug concentration [3]. The barrier is created by endothelial cells and a number of tight junctions that tighten up the overall structure and control the passive diffusion rate of solutes through the paracellular space. Potential drug candidates have to comply with certain criteria to permeate through the BBB ($\log P$ 2–5, PSA < 90, HBD < 3, and MW < 450) [4]. Transport proteins and receptors present at both sides of the BBB supply the brain with large molecules (e.g., insulin). Some important plasma proteins (e.g., albumin) can be transported via transcytosis [5–8]. A significant hurdle for targeting drugs to the brain is the presence of different efflux transporters in the BBB. Permeability glycoprotein (P-gp) is considered the most important among them and pumps the drugs back into the blood stream, which results in their restricted distribution or complete absence in the brain [9].

Electronic supplementary material The online version of this article (<https://doi.org/10.1007/s00216-018-0955-4>) contains supplementary material, which is available to authorized users.

✉ Deirdre Cabooter
deirdre.cabooter@kuleuven.be

¹ Pharmaceutical Analysis, Department of Pharmaceutical and Pharmacological Sciences, University of Leuven (KU Leuven), Herestraat 49, 3000 Leuven, Belgium

² Molecular Biodiscovery, Department of Pharmaceutical and Pharmacological Sciences, University of Leuven (KU Leuven), Herestraat 49, 3000 Leuven, Belgium

ADME (absorption, distribution, metabolism, and excretion) studies are performed to examine and predict drug behavior in the human body. Different models are currently available to investigate the BBB permeability of pharmaceutical compounds. However, none of these models seem to be generally adopted in the pharmaceutical industry. *In silico* models (e.g., QSAR) are cheap, fast, and do not require expensive lab work or clinical trials. However, they rely on *in vivo* data sets, the availability of which might be limited at the beginning of the drug discovery phase [10]. Parallel artificial membrane permeability assays (PAMPA) can be used as support tools for *in silico* models. These models show good predictability and high throughput [11, 12], but do not exhibit efflux transporters present in endothelial cells. Brain capillaries and endothelial *in vitro* cell lines are also often utilized, but their major drawback is the lack of complexity as encountered in the whole organism. This results into differences in expression levels of P-gp and Pg-p downregulation, as well as poor tightness of monolayer models leading to possible misinterpretation of the obtained outcomes [13–15]. In general, both *in silico* and *in vitro* outcomes have to be confirmed by *in vivo* experiments. The available mammalian models are intrinsically low-throughput and besides their insufficient time-cost-yield, the deteriorating public opinion on animal experiments has led to an increased use of non-warm-blooded animals. Particularly grasshopper and drosophila flies have been successfully shown to possess a BBB functionally similar to mammals [16, 17]. A significant weakness of all insect models is their exoskeleton consisting of chitin, excluding the topical administration route from possible administration options. Hence, there is still a demand for high-throughput vertebrate models.

Zebrafish (*Danio rerio*) is a small vertebrate animal model, which has become highly popular in biomedical research. The strength of this *in vivo* model relies on its high genetic, physiologic, and pharmacologic homology to humans [18–20]. This model animal is highly amenable to medium/high-throughput screening, as only one single adult pair can produce up to 200–300 eggs/week, resulting in a continuous supply of large numbers of eggs/embryos during experiments. Moreover, the developing zebrafish larvae have a size of 3–4 mm; thus, experiments can easily be performed by immersing the zebrafish in microtiter plates containing a suitable medium spiked with the compound of interest. Due to the small size of the zebrafish larvae, only microgram amounts of compound are required for this type of experiments, avoiding the loss of expensive lead compounds during early stages of drug development. An assessment of internal concentrations can be used to better understand ADME properties of pharmaceuticals in the early stages of drug discovery [21]. HPLC (high-performance liquid chromatography) and its miniaturized derivative techniques coupled to suitable types of detectors can be used to quantify small amounts of chemicals absorbed by the fish. Liquid chromatography (LC) has been reported frequently for the determination of internal concentrations of small

molecules, such as pharmaceuticals, pesticides, and metabolites in whole zebrafish [20, 22–30].

Several studies have been performed on the BBB of *Danio rerio*. It has been shown that zebrafish possess a similar CNS morphology to mammals, whereby the macro-organization of the brain and its cellular structure have been studied [31]. A size-dependent exclusion mechanism was demonstrated by analyzing the distribution of HRP (44 kDa) and sulfo-NHS-Biotin (0.443 kDa) injected into the heart. HRP was retained in cerebral vessels, but the smaller Sulfo-NHS-Biotin could diffuse into the brain [32]. It has also been shown that adult zebrafish express tight junction proteins in the endothelial vascular cells within the brain [32]. Tight junctions are however not present in sufficient numbers to tighten up the BBB at the moment the embryo breaks through the hull of the egg. The BBB undergoes gradual development until being fully matured and tight by 10 dpf (days post fertilization) [20].

The distribution of several drugs into the brain of zebrafish has so far been studied using adult zebrafish only (90 dpf or more). These fish were administered with the drugs of interest using intramuscular injection [33] or oral gavaging [34, 35]. Although brain dissection is more straightforward to perform in adult zebrafish, oral gavaging and intramuscular injection techniques are not as amenable to high-throughput analysis as immersion in well plates. Sufficient time and maintenance costs also need to be foreseen to grow the zebrafish to an adult age (> 90 dpf versus 10 dpf for zebrafish larvae). One study investigated drug uptake in the brain of zebrafish larvae (3–10 dpf) after immersion, but considered the whole head of the zebrafish for brain analysis, since brain dissection was considered impossible due to the small size of the zebrafish. Whole-head samples therefore also contained non-CNS tissue such as skin, bone, muscle, gills, eyes, and blood that can bias an accurate assessment of the actual drug uptake in the brain [20]. The main goal of this study therefore was to take a more precise approach by investigating the distribution of 7 drugs displaying different physicochemical properties and known to have a variable penetration through the BBB of mammals [36–40], into the actual brain of the fish. For this purpose, a technique allowing the extraction of the pure brain of zebrafish larvae (10 dpf) was developed using a fluorescence microscope and ultra-fine end tweezers. To analyze the small sample volumes, capillary LC-UV was used to benefit from the reduced inner diameter of the column leading to lower chromatographic dilution and hence lower detection limits [41]. This technique proved to be sensitive enough to quantify the concentrations of the drugs considered in this study in pooled zebrafish samples ($n = 6$). To the best of our knowledge, this is the first study wherein the pure brain of zebrafish larvae is extracted and subsequently analyzed using a capillary LC methodology to determine the uptake of pharmaceuticals in zebrafish brain.

Materials and methods

Chemicals

Carbamazepine (CBZ), haloperidol (HLP), and desipramine (DSP) were purchased from Alpha Pharma (Zwevegem, Belgium); bupropion (BUP), trazodone (TRA), and warfarin (WAF) were from Sigma-Aldrich (Steinheim, Germany); and quinidine (QND) from TCI (Zwijndrecht, Belgium). The physicochemical properties of the compounds were calculated using the ChemAxon software imbedded in MarvinSketch 16.12.12, are shown in Table 1, and largely comply with the criteria to permeate through the BBB as stated in the “Introduction” section. In fact, all compounds are known to display some degree of penetration through the BBB of mammals [36–40]. All physicochemical values were determined at pH = 7.6, corresponding to the pH value wherein the zebrafish were maintained (see the “Zebrafish housing and breeding” section).

Formic acid, methanol (MeOH), and acetonitrile (ACN) were from VWR (Leuven, Belgium), ethanol was from Fischer Scientific (Loughborough, UK), and ammonium formate from Fluka (Buchs, Switzerland). All reagents were MS-grade. pH modifications were done with a Metrohm pH meter (Antwerp, Belgium). Polystyrene 24-well plates (Falcon®) were from VWR. Weighing experiments were performed using a Sartorius Cubis Ultramicrobalance (Göttingen, Germany).

DSP and WAF were prepared as 5 mM stock solutions in DMSO (Sigma-Aldrich), while BUP, TRA, and QND were dissolved in ultrapure water in a concentration of 5 mM, CBZ was dissolved in acetonitrile (5 mM), and HLP was dissolved in ethanol (5 mM). All stock solutions were stored at –80 °C. Ultrapure water was produced using a Millipore Milli-Q Gradient System (Milford, MA, USA).

Table 1 Physicochemical properties of the compounds investigated in this study

Compound	PSA (pH = 7.6)	Log <i>D</i> (pH = 7.6)	HBD (pH = 7.6)	MW (g/mol)
CBZ	46.33	3.22	2.00	236
TRA	42.39	4.66	0.24	372
WAF	66.43	0.72	0.01	308
BUP	33.68	2.04	1.81	240
DSP	19.85	1.25	2.00	266
QND	46.79	0.86	1.97	324
HLP	41.74	2.5	1.74	376

PSA polar surface area, Log *D* distribution coefficient, HBD number of hydrogen bond donors, MW molecular weight

Zebrafish housing and breeding

Animal experiments were approved by the Animal Ethical Committee of the University of Leuven (approval no. P007/2016). Adult zebrafish specimen (strain TG898) was kept under standard aquaculture conditions (temperature of 28.0 °C and light/dark cycle of 14/10 h). Petri dishes containing Danieau medium (1.5 mM HEPES, pH 7.6, 17.4 mM NaCl, 0.21 mM KCl, 0.12 mM MgSO₄, and 0.18 mM Ca(NO₃)₂) and placed in an incubator were used to maintain the freshly laid fertilized eggs and grow the juvenile fish to the age of 10 days. All fish were visually screened for possible malformations and only healthy animals were used for further experiments.

Instrumental analysis

An UltiMate 3000 series RSLC nano system from Dionex (Amsterdam, The Netherlands) was used for analytical experiments. The system consisted of two pumps (a binary capillary/nano UHPLC pump and a UHPLC loading pump), a degasser, an autosampler, a thermostatted column compartment, and a variable wavelength detector VWD-3400RS with a 45-nL Z-shaped flow cell. Detection was performed at 254 nm at an acquisition rate of 25 Hz. System operation and data acquisition were done using the Chromeleon software 6.80 (Dionex).

A reversed-phase Acclaim Pepmap RSLC C18 capillary column (150 mm × 300 μm, *d_p* = 2 μm) in combination with a C18 Pepmap100 μ-precolumn (5 mm × 300 μm, *d_p* = 5 μm) was used for all chromatographic separations. Both columns were from Thermo Fischer Scientific (Erembodegem, Belgium) and were thermostatted at 40 °C. The temperature of the autosampler containing the samples was set at 5 °C. Different injection volumes (*V_{inj}*) of 0.5, 1, 2, and 5 μL were evaluated. Mobile phases consisted of 10 mM ammonium formate adjusted to pH 2.8 using formic acid (A) and 10:90 (v/v) water/ACN with 0.8% formic acid (B). Gradient elution was performed from 95:5 (v/v) A/B to 18:82 (v/v) A/B at a flow rate of 5 μL/min. Different gradient times between 25 and 30 min were evaluated.

Linearity, LLOQ, matrix effects

Compounds of interest were spiked into a mobile phase-like solution (94:6 (v/v) H₂O/ACN) at a minimum of 8 concentrations. Each concentration was injected three times consecutively and the average obtained peak areas were plotted versus the concentration. The lower limit of quantification (LLOQ) was defined as the lowest concentration point for which a signal-to-noise ratio (S/N) ≥ 10 was obtained, while the RSD value was < 20%. Matrix effects were investigated by comparing the slopes of the linearity curves obtained in matrix solution (by spiking the compounds into evaporated blank

samples of trunks and brains of 10-day old zebrafish (six fish per experiment, $n = 6$), see the “[Sample preparation](#)” section) at 3 different concentration levels, to those obtained for standard solutions of the compounds of interest dissolved in 94:6 (v/v) H_2O/ACN .

Precision, accuracy, and specificity

Interday precision was determined for three different concentrations (0.016 $\mu\text{g/mL}$ —low-range concentration LRC, 1 $\mu\text{g/mL}$ —mid-range concentration MRC, and 2 $\mu\text{g/mL}$ —higher limit of quantification HLQ), each prepared separately on three consecutive days and each injected three times ($n = 3$). Simultaneously to those measurements, intraday precision was investigated by performing three additional injections on 1 day at LRC and HLQ, resulting in a total of six injections on the same day ($n = 6$) for these concentrations. Interday and intraday precision were performed with compounds spiked into the evaporated blank samples (both brains and trunks) of 10-days-old zebrafish, using six fish ($n = 6$) per experiment (see the “[Sample preparation](#)” section).

Intraday and interday accuracy were investigated by spiking six blank zebrafish brain and trunk samples ($n = 6$) per concentration with the compounds of interest at concentrations corresponding to 3 times the LRC, 37.5% the HLQ, and 75% the HLQ, respectively. Bias percentage values of the spiked samples were calculated using the following formula:

$$\text{Bias [\%]} = \frac{\text{concentration found} - \text{concentration spiked}}{\text{concentration spiked}} \times 100 \quad (1)$$

Method specificity was evaluated by comparing brain and trunk chromatograms obtained from blank zebrafish samples, blank zebrafish samples spiked with the compounds of interest, and zebrafish samples obtained after immersion in medium spiked with the compounds of interest.

Sample preparation

The procedure of compound extraction from the whole body of the fish has been described somewhere else in detail [42]. Briefly, zebrafish were sacrificed by flushing them with 25 mL ice-cold ultrapure water on a 200- μm sieve and subsequently processed as mentioned in the “[Brain uptake experiments](#)” section. Six dissected brains or trunks were pooled together in one 1.5-mL Eppendorf® Safe-Lock® tube pre-filled with acid washed glass beads (diameter 710–1180 μm , Sigma-Aldrich) and 270 μL of extraction medium (1:2 water/MeOH containing 0.1% v/v formic acid) were added into each tube. The homogenization was performed by ultrasonication (Diagenode Bioruptor Plus, Seraing, Belgium) at $+4^\circ$ using the high energy input setting. The overall treatment time was 15 min spread over 30 cycles of 30 s with pauses of 30 s in-between. Afterwards, these samples were centrifuged at $14.1 \times 1000g$ (Eppendorf Mini Spin Plus, Hamburg, Germany) for 15 min and 200 μL of supernatant was transferred to an empty Eppendorf tube (1.5 mL) and stored on ice. Subsequently, all samples were placed in a vacuum oven (Model 1410, Sheldon Manufacturing Inc., Cornelius, OR, USA) and evaporated until dryness at $+45^\circ\text{C}$ during 45 min. The samples were then reconstituted in a mobile phase-like solution (94:6 (v/v) H_2O/ACN), vortexed for 5 s, re-suspended at least 3 times with a micropipette, and sonicated (Branson 3510, Danbury, CT, USA) for 15 min. Specifically for this study, the reconstitution volume was chosen in such a way that the linearity range of the method was not exceeded (Table 2). To avoid clogging of the small I.D. capillary LC column, trunk samples were additionally filtered prior to analysis. To investigate whether any significant compound loss occurred during filtering, the amount of compound adsorbed onto the filter during the filtering process was measured using three types of filters: regenerated cellulose (RC), polytetrafluoroethylene (PTFE), and polyamide (PA). Based on the obtained recoveries, trunk-derived samples

Table 2 Reconstitution volumes for brain (B) and trunk (T) samples, including filter types used for the trunk samples. The recoveries obtained for the filters are also given, together with the RSD values on these filter recoveries ($n = 3$)

Compound	Reconstitution volume B (μL)	Reconstitution volume T (μL)	Filter type T	Filter recovery (%)	RSD (%)
BUP	40	500	PTFE	90.9	5.3
CBZ	50	500	RC	95.5	2.9
DSP	40	250	PTFE	88.3	6.9
TRA	50	500	PTFE	82.1	6.5
QND	40	500	PTFE	82.5	7.8
HLP	40	500	PTFE	71.3	14.3
WAF	50	500	RC	96.0	0.5

RC regenerated celluloses, PTFE polytetrafluoroethylene

were filtered through 0.2 μm Minisart RC 4 (Sartorius, Stonehouse, UK) or 0.2 μm PTFE (General Electrics, Buckinghamshire, UK) filters (Table 2, only the best filter types are shown). Finally, samples were transferred into glass vials (Supelco, Bellefonte, PA, USA) with 200 or 400 μL glass inserts (Supelco) for further analysis on capillary UHPLC-UV.

Method recovery

Method recovery was determined at two concentration levels (0.05 and 1 $\mu\text{g}/\text{mL}$) for each compound and both brain- and trunk-derived samples separately. First, a set of evaporated samples was prepared drug-free and then spiked with each compound during the reconstitution step ($V_{\text{reconstitution}} = 200 \mu\text{L}$). The obtained response A_{x1} (area of compound), which was unaffected by the sample preparation, still indicated possible influences of the matrix on the chromatographic separation. A second set of samples underwent the described preparation procedure (see the “Sample preparation” section) with an equal reconstitution volume of 200 μL , whereby the extraction medium was spiked with the same concentration as in A_{x1} . The response A_{x2} obtained for this second set of samples indicated the compound loss due to the sample preparation. Method recovery was subsequently calculated as follows:

$$\text{Recovery [\%]} = 100\% \times \frac{A_{x2}}{A_{x1}} \quad (2)$$

Measuring of dry weight

A common approach to express the whole-body uptake of a pharmaceutical agent is to establish a relation between the concentration taken up by the fish and the body weight of the fish [20, 29]. In this study, the body weight of the fish was expressed as the dry weight, since this was considered to be more accurate, as no water film sticking to the skin of the animals would bias the weighting. Before measuring the dry weight, zebrafish were sacrificed with ice-cold water, then brains were extracted as described in the “Brain uptake experiments” section. The weight was determined by first heating a glass dish at 105 $^{\circ}\text{C}$ followed by cooling at room temperature in a desiccator and repeating this procedure until a constant mass (m_1) was obtained. Subsequently, 40 trunks or 40 brains were added to the glass dish and dried following the same procedure until constant mass (m_2). The initial mass m_1 was subtracted from the final mass m_2 to obtain the dry weight.

Toxicity experiments

Survival of the zebrafish larvae was ensured by determining the maximum tolerated concentrations (MTC) prior to the uptake experiments. For this purpose, 7 different concentrations per compound (0.8–50 μM) were investigated in a 96-well plate. Each fish was put into a single well and six fish were monitored per concentration. The vitality of the fish was examined after 1 h of incubation at + 28 $^{\circ}\text{C}$ during the light phase. A concentration

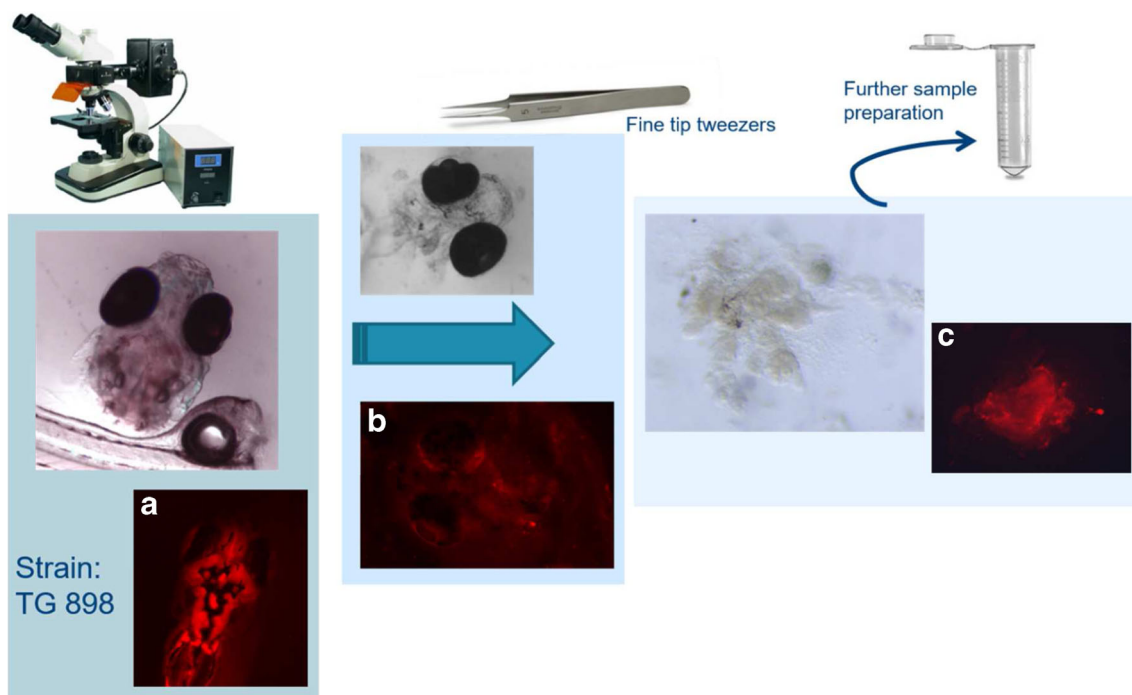


Fig. 1 Workflow of brain extraction. **a** The intact head, including the brain. **b** The empty head after extracting the brain. **c** The brain extracted from the head. For further details, the reader is referred to the text (“Brain uptake experiments” section)

was considered to be non-toxic, if not more than 1 fish died during the treatment while all control fish (i.e., fish that were not incubated with compounds) were still alive.

Brain uptake experiments

To investigate the concentration of the different compounds in the brain after immersion, a brain dissection technique was developed to remove the brain from the body without compound loss. For this purpose, the body of an euthanized larva was carefully separated from the head under a Leica MZ 10F microscope (Leica Microsystems, Wetzlar, Germany) by applying a cut with sharp-tipped Dumont Nr.5 tweezers (WPI, Hitchin, UK) between the end of the opercle and the pectoral fins. Subsequently, the brain was removed using ultra-fine end Dumont Nr. 5SF tweezers (WPI). Figure 1 demonstrates the process of brain extraction. The top pictures visualize the brain extraction using an optical microscope, while the bottom pictures illustrate the removal of the brain under a fluorescence microscope. For the latter experiments, a special strain (TG898) of zebrafish that exhibits brain fluorescence was used to check the integrity of the brain after removal.

Uptake experiments were performed in the wells of a 24-well plate filled with 1 mL of Danieau medium spiked with one compound of interest at the MTC. Three fish ($n = 3$) were placed into a single well and incubated for 1 h at +28 °C during the light phase. Brains from incubated fish from 2 well plates ($n = 6$) were pooled into one Eppendorf® tube for further processing (see the “Sample preparation” section). The rest of the bodies, further referred to as trunks, were collected and pooled in the same way into one Eppendorf® tube. A second 24-well plate spiked with the compounds of interest at the MTC was prepared to determine the amount of compound sticking to the skin of the fish. Hereby, zebrafish larvae were immersed into the spiked medium and immediately transferred on a sieve for further sample preparation. The final uptake was obtained by subtracting

the value of compound sticking to the skin of the fish from the uptake measured after 1 h in the trunk of the fish, while also taking recovery into account.

Results and discussion

Optimization of chromatographic separation

A gradient method was developed for the 7 compounds under investigation, wherein the percentage of mobile phase B increased from 5 to 90% in gradient times ranging between 25 and 30 min. For a gradient time of 25 min, co-elution between CBZ and an impurity was observed. The gradient time was therefore increased to 28 min with a decrease in gradient slope steepness between 12.5 and 21 min resulting in the successful separation of all compounds (Fig. 2). In the final method (Table S1, see the Electronic Supplementary Material, ESM), an isocratic hold (t_{iso}) of 0.5 min was introduced as well to better focus the early eluting compounds on the top of the column and to obtain sharper peak shapes.

Optimization of injection volume

In order to find the best compromise between sensitivity and extra-column band broadening, different injection volumes (0.5, 1, 2, and 5 μL) were investigated for the optimized gradient separation (ESM Fig. S1). The concentrations of the test compounds were adapted to the injection volume in such a way that the same amount of compound was each time injected onto the column. In general, a dramatic decrease in sensitivity was observed at $V_{inj} = 5 \mu\text{L}$ for all compounds, since such a large injection volume increased the extra-column band broadening significantly (note that the void volume of the column is approximately $V_0 = 4 \mu\text{L}$). The signal-to-noise ratio of QND, BUP, TRA, HLP, and DSP (ESM Fig.

Fig. 2 Optimized gradient separation of the 7 target compounds ($V_{inj} = 1 \mu\text{L}$). Column: Acclaim Pepmap RSLC C18 capillary column (150 mm \times 300 μm , $d_p = 2 \mu\text{m}$) and $T_{column} = 40 \text{ }^\circ\text{C}$. Mobile phase: 10 mM ammonium formate with formic acid (pH 2.8) (mobile phase A) and 10:90 (v/v) water/ACN with 0.8% formic acid (mobile phase B). The flow rate was 5 $\mu\text{L}/\text{min}$ and the conditions of the gradient elution are given in Table S1 (see the ESM)

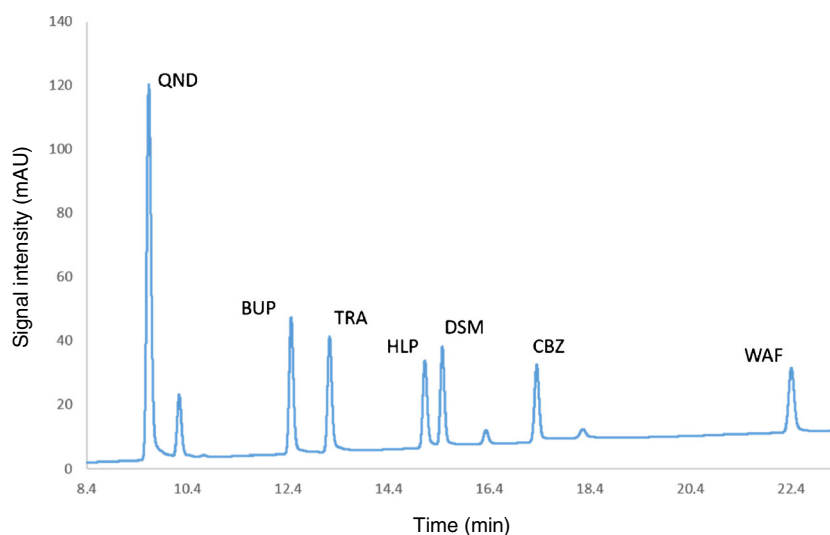


Table 3 Determined linear range, lower limit of quantification (LLOQ), linear regression coefficient and matrix effects

Compound	Linear range ($\mu\text{g/mL}$)	LLOQ ($\mu\text{g/mL}$)	R^2	Matrix effects (%)	
				Brain	Trunk
BUP	0.008–2	0.008	0.9997	106	98
CBZ	0.016–2	0.016	0.9993	102	100
DSP	0.003–2	0.003	0.9979	114	88
HLP	0.003–2	0.003	0.9972	110	95
TRA	0.016–2	0.016	0.9999	112	99
QND	0.002–2	0.002	0.9996	109	100
WAF	0.008–2	0.008	0.9984	103	101

S1a–e) was also clearly influenced by an injection volume of 2 μL , yet not to the extent of $V_{\text{inj}} = 5 \mu\text{L}$. The most retained compounds CBZ and WAF (ESM Fig. S1f, g) did not show any signal-to-noise changes for injection volumes ranging between 0.5 and 2 μL , due to their higher retention volume. Injection volumes of 0.5 and 1 μL did not show any significant differences in peak shape for all compounds; therefore, a $V_{\text{inj}} = 1 \mu\text{L}$ was determined to be the most suitable for all further experiments.

Linearity, LLOQ, matrix effects

In a previous study using a 2.1-mm ID UHPLC column in combination with a triple quadrupole mass spectrometer [42], it was demonstrated that the whole-body uptake of pharmaceuticals in zebrafish can be measured using a single fish per experiment. Uptake values measured in [34], ranged between 0.002 and 0.094 $\mu\text{g/mL}$. LLOQ values measured with the capillary UHPLC-UV set-up used in this study were determined to range between 0.002 and 0.016 $\mu\text{g/mL}$ for all compounds (Table 3). Since the uptake values measured in the brain were expected to be lower compared to the uptake values in the whole body of a fish, it was decided to pool six fish in this study to increase the available amount of compound per experiment. Calibration curves measured between the LLOQ and 2 $\mu\text{g/mL}$ showed good linearity with R^2 values

above 0.9972 (Table 3). Matrix effects were measured separately for dissected brain and trunk samples at 3 concentration points (0.016, 1, and 2 $\mu\text{g/mL}$). The comparison of the linearity slopes obtained in biological samples and mobile phase revealed no significant matrix effects, with a ratio ranging between 102 and 114% for brain samples and between 88 and 101% for trunk samples. All values complied with regulatory guidelines [43].

Precision, accuracy, and specificity

Intraday precision of the method was evaluated by injecting the concentrations corresponding with the LRC and HLQ six times ($n = 6$). Interday precision was calculated from the values obtained on 3 different days by injecting the concentrations corresponding with the LRC, MRC, and HLQ three times ($n = 3$). Experimental data obtained for brain-derived samples are shown in Table 4 and display RSD values between 0.7 and 9.8%. All values complied with the maximum limit of 15% set by the regulatory guidelines [43]. Table 5 shows the values for intra- and interday precision for the trunk-derived samples. Since the RSD values ranged between 0.5 and 9.3%, all values complied with the regulatory guidelines (RSD < 15%).

Inter- and intraday accuracy values for brain-derived samples are shown in Table S2 in the ESM. The obtained values complied with regulatory guidelines being in general not

Table 4 Intra- and interday precision for brain-derived samples displayed as RSD values

Compound	Intraday precision ($n = 6$)		Interday precision ($n = 9$)		
	LRC (%)	HLQ (%)	LRC (%)	MRC (%)	HLQ (%)
BUP	2.3	0.8	1.7	1.9	2.4
CBZ	5.2	1.4	3.3	1.1	1.9
DSP	6.1	3.5	5.3	3.7	2.9
HLP	9.8	2.9	5.7	3.1	2.5
TRA	2.6	2.8	1.7	1.7	2.1
QND	1.8	2.2	2.9	2.0	3.7
WAF	3.9	0.7	1.9	0.7	1.6

LRC low-range concentration, MRC mid-range concentration, HLQ highest limit of quantification

Table 5 Intra- and interday precision for trunk-derived samples displayed as RSD values

Compound	Intraday precision (<i>n</i> = 6)		Interday precision (<i>n</i> = 9)		
	LRC (%)	HLQ (%)	LRC (%)	MRC (%)	HLQ (%)
BUP	1.6	0.6	1.3	1.0	0.5
CBZ	9.3	0.5	6.3	0.6	1.4
DSP	2.8	1.5	3.0	1.5	4.0
HLP	8.0	1.1	4.8	1.8	2.9
TRA	3.6	0.9	2.5	1.1	1.9
QND	7.0	0.5	3.2	0.7	0.8
WAF	3.2	0.6	3.6	0.6	1.2

LRC low-range concentration, MRC mid-range concentration, HLQ highest limit of quantification

higher than the recommended maximum for relative bias of 15%. Accuracy values measured for the trunk-derived samples (ESM Table S3) largely complied with the regulatory guidelines with only the interday relative bias of DSP (19.49%) and CBZ (18.20%) displaying values slightly over the margin of 15%. The interday and intraday precision of the accuracy measurements did not exceed the acceptable RSD limit of 15% for both brain- and trunk-derived samples.

Chromatograms of blank zebrafish samples, blank zebrafish samples spiked with the compound of interest, and zebrafish samples obtained after immersion of the fish in medium spiked with the compound of interest are shown in the ESM in Figs. S2–S8 for brain-derived samples and in Figs. S9–S15 for trunk-derived samples. Interfering peaks from endogenous compounds are absent at the retention times of the investigated pharmaceuticals, demonstrating the specificity of the method. Although an impurity peak was observed close to WAF, it was still clearly separated and did not influence the measurements.

Method recovery

Recoveries were determined for all compounds at two concentrations of 0.05 and 1 µg/mL for both brain and trunk extracts. Recoveries of brain samples for both concentrations

were largely the same ranging between 75.6 and 116.8% for the different compounds (Table 6), while the recoveries for the trunk samples were in general slightly lower ranging between 73.7 and 99.1% which can be explained by the use of the PTFE and RC filters retaining small amounts of compounds during the sample filtration (Table 2). Although few recoveries were somewhat lower than the 80–120% margin stated by regulatory guidelines [43], these values were still considered acceptable since the RSD values were relatively low, in general not exceeding 11.2%.

Measuring of dry weight

The dry weight averaged over 40 fish, led to a dry weight of 7 µg for 1 dissected brain and 24 µg for the rest of the fish body. This means an overall dry weight of 31 µg for a whole fish. With a reported value of 330 µg wet weight for 1 fish [20], the obtained values indicate that more than 91% of the fish consists of water.

Toxicity experiments

No intoxication effects were recorded for BUP, CBZ, QND, TRA, and WAF over the whole range of concentrations and duration of treatment (Table 7). Several anxiolytic pharmaceuticals

Table 6 Compound recoveries and their relative bias for brain and trunk samples

Compound	Brain				Trunk			
	Recovery (%)	RSD (%)	Recovery (%)	RSD (%)	Recovery (%)	RSD (%)	Recovery (%)	RSD (%)
	0.05 µg/mL		1 µg/ml		0.05 µg/mL		1 µg/ml	
BUP	81.1	3.5	80.6	2.1	90.1	2.2	86.5	1.3
CBZ	86.1	1.0	84.0	8.8	92.5	0.8	86.6	1.9
DSP	84.9	3.6	77.5	3.1	75.8	11.2	83.0	7.4
HLP	116.8	4.0	89.9	3.4	73.7	7.6	89.0	3.5
QND	85.8	6.1	84.0	7.6	83.9	5.2	91.3	5.8
TRA	75.6	2.0	79.3	8.7	81.1	8.5	90.9	5.2
WAF	101.0	5.3	96.0	8.6	99.1	3.0	97.0	6.0

Table 7 Maximum tolerated concentrations for zebrafish ($n = 6$) and solubility of tested compounds

Compound	MTC ($\mu\text{g/mL}$) 1 h	Solubility water ($\mu\text{g/mL}$)
BUP	> 12.0	312×10^3
CBZ	> 11.8	17.7
DSP	6.65	145.0
HLP	2.35	14.0
QND	> 16.2	334.0
TRA	> 18.6	290.0
WAF	> 15.4	17.0

were recently associated with the induction of oxidative stress [44], possibly explaining the toxicity of DSP in the range between 6.65 and 13.30 $\mu\text{g/mL}$. The obtained MTC value for HLP was slightly lower than previously reported in the literature by Fleming et al. (2.35 versus 7.5 $\mu\text{g/mL}$) [20]. A possible explanation might be the use of the more toxic solvent ethanol in this study compared to DMSO in the Fleming study [20]. In general, all MTC values were well under their solubility limit in water (Table 7) indicating that no solubility problems were to be expected at these MTC values.

Brain uptake experiments

Brain and trunk uptake values were measured by preparing six fish ($n = 6$) as described earlier in the “Sample preparation” section. To measure the actual compound uptake in the brain, the brain was carefully removed from the body. By using a zebrafish strain exhibiting red fluorescence of the brain (TG898), it was possible to distinguish between the actual brain and the head of the fish (Fig. 1). Figure 1a shows the intact head of the fish, including the brain. Figure 1b shows the remaining head, after removing the brain. The intensity of the fluorescence is clearly lower in Fig. 1b compared to Fig. 1a, indicating that the brain has been effectively removed. Figure 1c shows the brain after removal. Again, the fluorescence signal helps to assess whether the brain is still intact after removal. The obtained uptake concentration was corrected for matrix effects and compound recovery. Based

Table 8 Uptake values for the trunk (T) and the brain (B) of the fish with corresponding brain-to-trunk (B/T) ratio

Comp.	Uptake (T) ($\mu\text{g/g}$)	RSD (%)	Uptake (B) ($\mu\text{g/g}$)	RSD (%)	B/T ratio	RSD (%)
CBZ	120.9	6.5	113.8	15.5	0.9	22.9
TRA	1794.3	3.0	735.1	16.5	0.4	24.2
WAF	59.4	16.9	33.7	14.4	0.6	34.3
BUP	404.2	11.7	130.3	7.5	0.3	10.8
DSP	11.9	25.7	14.3	2.5	1.2	31.7
QND	31.9	0.7	13.2	11.4	0.4	14.3
HLP	95.2	11.9	53.3	16.6	0.6	7.6

on the principle of brain-to-plasma ratio usually applied for mammals [13], the brain-to-trunk ratio was used for the evaluation of brain permeation of the compounds. Typical values used in literature are 0.3–0.5 for sufficient access to the central nervous system (CNS), > 1 for freely crossing across the BBB and < 0.1 for drugs which are unable to enter the CNS. It is obvious that at ratios < 1.0 some exclusion processes occur. In any case, these general values have to be seen in the context of concentration-dependent compound efficaciousness.

First, it has to be noted that the obtained trunk uptake concentrations (Table 8) are remarkably close to the ones measured for the whole-body uptake in a previous study [42]. As these experiments were carried out on different types of LC systems (UPLC versus capillary UHPLC) using different types of detectors (mass spectrometer and UV detector), this indicates that the developed methodology is robust and repeatable. Furthermore, a loose correlation ($R^2 = 0.64$) between lipophilicity and compound uptake in the trunk can be observed (Fig. 3a), whereby the compounds with the lowest log D values (desipramine, quinidine, and warfarin) exhibit the lowest trunk uptake (11.9, 13.9, and 59.4 $\mu\text{g/g}$) and trazodone, the compound with the highest log D value, is taken up the most (1794.3 $\mu\text{g/g}$). This correlation between uptake and lipophilicity was already observed in several other studies [20, 23, 42] and suggests that absorption in zebrafish is largely dominated by passive diffusion. No clear correlation could be observed between trunk uptake and other physicochemical properties (PSA, MW, HBD) (Fig. 3b–d), possibly due to the fact that their range was not sufficiently large to obtain a clear correlation.

The trends between measured brain uptake in relation to the compounds' physicochemical properties were somehow similar to the trends observed for the trunk (Fig. 4a). The lowest uptake was shown for desipramine, quinidine, and warfarin (14.3, 13.2, and 33.7 $\mu\text{g/g}$, respectively) exhibiting the lowest log D values, while trazodone showed the highest brain uptake (735.1 $\mu\text{g/g}$). The linear correlation between brain uptake and log D was stronger ($R^2 = 0.71$) compared to the one observed for trunk uptake, again indicating passive diffusion as an important mechanism for BBB crossing. Also, no correlation could be confirmed between detected compound and polar surface area, molecular weight, or number of hydrogen bond donors (Fig. 4b–d).

Fig. 3 Influence of **a** the lipophilicity ($\log D$ at $\text{pH} = 7.6$), **b** the polar surface area (PSA at $\text{pH} = 7.6$), **c** the molecular weight (MW), and **d** the number of hydrogen bond donors (HBD) on the trunk uptake of 10-day-old fish. Legend: ■ BUP; ▲ CBZ; ◇ DSP; ◆ HLP; □ TRA; △ QND; ● WAF

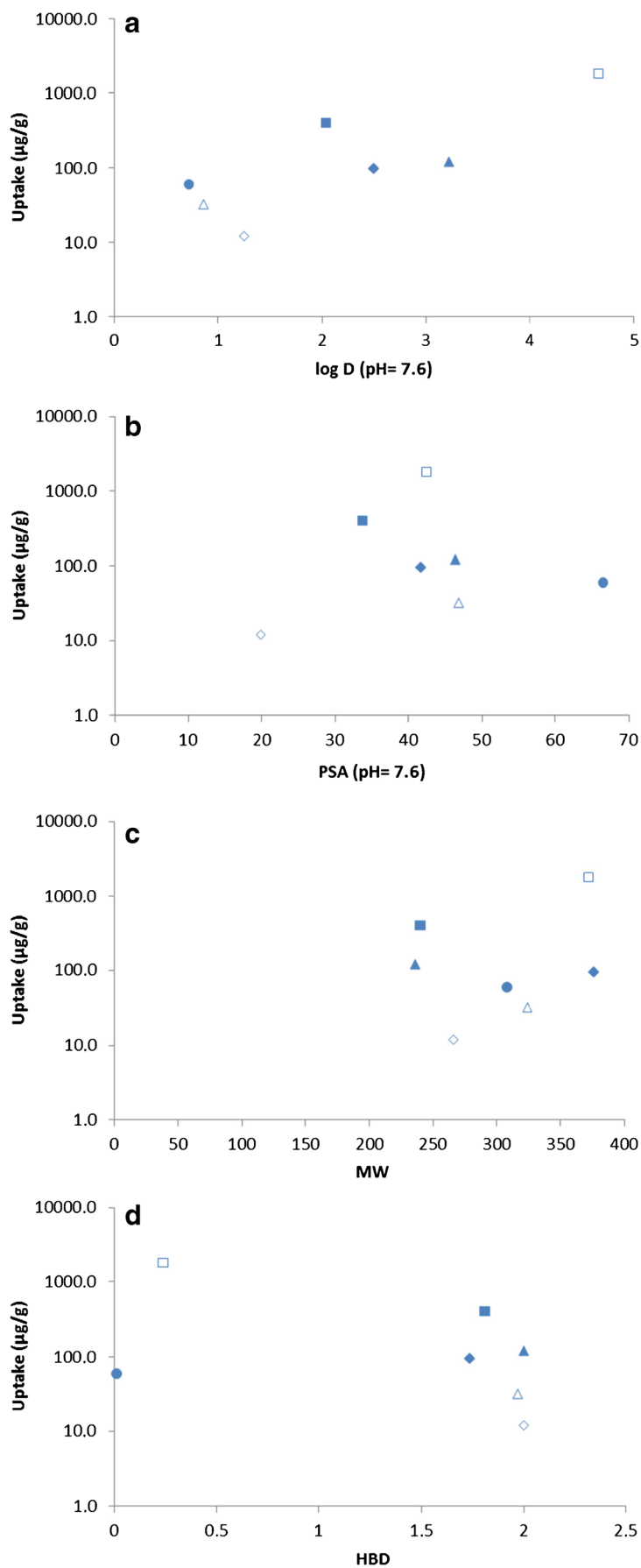
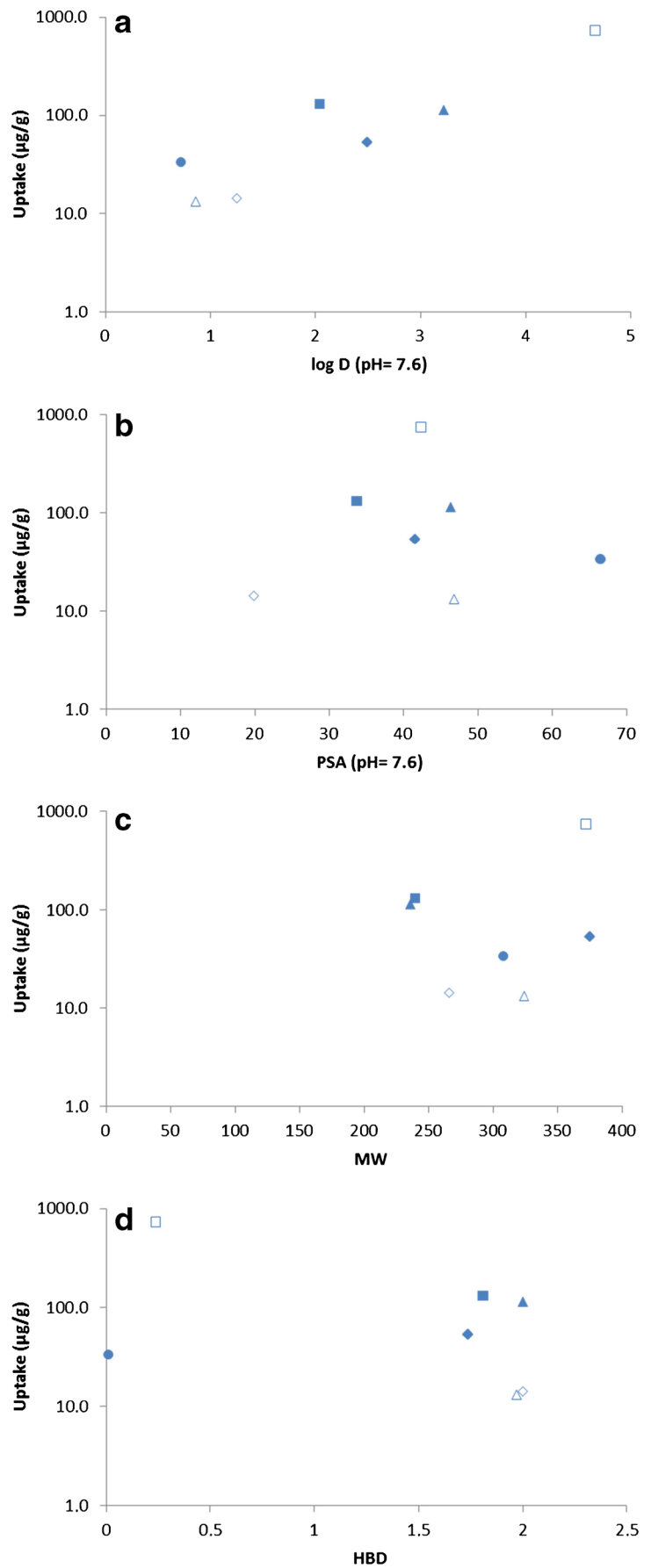


Fig. 4 Influence of **a** the lipophilicity ($\log D$ at $\text{pH} = 7.6$), **b** the polar surface area (PSA at $\text{pH} = 7.6$), **c** the molecular weight (MW), and **d** the number of hydrogen bond donors (HBD) on the brain uptake of 10-day-old fish. Legend: ■ BUP; ▲ CBZ; ◇ DSP; ◆ HLP; □ TRA; △ QND; ● WAF



The RSD values (Table 8) between 0.7 and 25.7% for trunk uptake and between 2.5 and 16.6% for brain uptake moreover demonstrated the good repeatability of the developed brain extraction and analysis procedure.

An important criterion for the decision whether a CNS-pharmaceutical should enter the next development stage is the brain-to-trunk (B/T) ratio. The B/T ratios of the investigated compounds ranged between 0.3 and 1.2, with a variation between 7.6 and 34.3%, showing good repeatability of the data.

Specifically, desipramine showed the highest B/T ratio of 1.2 indicating free access through the blood-brain barrier. Previous experiments in rat indicated an even higher blood-to-plasma (B/P) ratio of 1.6 to > 20, depending on the time of sampling due to differences in clearance rate in brain and plasma at different time points, and a strong accumulation of the compound in the brain of a rat [36]. Despite the difference in absolute B/T and B/P values, both *in vivo* models clearly indicate that desipramine freely crosses the BBB. Carbamazepine exhibited a B/T of 0.9 in zebrafish, whereby a rat study revealed a similar brain-to-plasma ratio of 0.74, suggesting CBZ is somewhat obstructed from entering the brain [37]. Haloperidol showed a B/T ratio of 0.6 in our study. It is the only compound that has already been investigated on the subject of BBB penetration in zebrafish and showed to have free accessibility (head-to-trunk ratio 1.1) in another study [20]. However, the experiments performed in [20] were conducted on the whole head, possibly being biased by a higher drug concentration in the head environment (blood/eyes) outside the brain. Warfarin was reported to exhibit a brain-to-plasma ratio of 0.49 in rat after 1 h of administration [38], while in this study, it showed a similar B/T ratio of 0.6 again indicating some accessibility restrictions.

Typical values for brain-to-plasma ratio of trazodone and bupropion are 1.4–6.0 (rat) [39] and 11.25 (guinea pig) [40]. Surprisingly, the determined brain distribution of trazodone (0.4) and bupropion (0.3) was relatively low, indicating a possible exclusion mechanism in the brain of the fish. Quinidine is frequently used to demonstrate the suitability of CNS models as it poorly crosses the blood-brain-barrier due to the efflux by Pg-p [10]. Nevertheless, a B/T ratio of 0.4 was detected for QND. On the one hand, the low ratio indicates some discrimination of the compound from the brain; on the other hand, TRA and BUP, which should be able to accumulate inside the brain, displayed similar B/T ratios to QND. Fleming et al. showed another compound which should be excluded from the brain (scopolamine *N*-butyl bromide) to exhibit a B/T ratio of 0.8 [20]. Possibly, Pg-p are oversaturated by the amount of QND present in blood, resulting in an increased uptake. The results show that the selective BBB in zebrafish brain is clearly present and can be demonstrated using the developed methodology. However, the exact mechanism cannot yet be completely understood and will need more extensive investigations in the future.

Conclusions

The current study presents a new method to extract the brain of zebrafish larvae (10 dpf) in an accurate and fast manner. Using two sharp-tipped tweezers and a fluorescence microscope, it is possible to perform the extraction without having to resort to expensive laser dissection equipment. This procedure is also less labor-intensive and requires only 2–5 min for the extraction of one brain. The use of capillary columns with a reduced ID in combination with UV detection was investigated for the evaluation of drug uptake in the brain of zebrafish larvae. To ensure sufficiently concentrated samples, the sample preparation procedure presented in an earlier publication [42] was applied using pooled samples of six zebrafish larvae for each single experiment.

The correlation between absorption of the compounds, its permeation through BBB, and the lipophilicity ($\log D$) of the compounds was confirmed. No obvious correlation could be observed between compound absorption or BBB permeation and other physicochemical factors such as molecular weight, polar surface area, and number of hydrogen bond donors. Although brain uptake could be measured precisely and the semipermeable nature of the BBB was demonstrated, the obtained brain-to-trunk ratios did not give a clear answer to whether zebrafish is a suitable high-throughput BBB model, since two compounds (bupropion, trazodone) that are known to cross the BBB of mammals freely exhibited the same B/T ratio as a compound that is usually discriminated from the access to the brain (quinidine).

Future experiments will be carried out on a more extensive set of compounds, considering more time points for the determination of the B/T ratio. Also, the activity and role of efflux pumps will be evaluated using P-gp blockers in a follow-up study.

Acknowledgements ARIADME, a European FP7 ITN Community's Seventh Framework Program under Grant Agreement No. 607517, is acknowledged for the financial support.

Compliance with ethical standards

All animal experiments were approved by the Animal Ethical Committee of the University of Leuven (approval no. P007/2016) and conducted in accordance with the Belgian and European laws, guidelines, and policies for animal experimentation, housing, and care (Belgian Royal Decree of 29 May 2013 and European Directive 2010/63/EU on the protection of animals used for scientific purposes of 20 October 2010).

Conflict of interest The authors declare that they have no conflict of interest.

References

1. Engelhardt B. Development of the blood-brain barrier. *Cell Tissue Res.* 2003;314:119–29. <https://doi.org/10.1007/s00441-003-0751-z>.
2. Pardridge WM. The blood-brain barrier: bottleneck in brain drug development. *NeuroRx.* 2005;2:3–14. <https://doi.org/10.1602/neurorx.2.1.3>.

3. Reichel A. Addressing central nervous system (CNS) penetration in drug discovery: basics and implications of the evolving new concept. *Chem Biodivers*. 2009;6:2030–49. <https://doi.org/10.1002/cbdv.200900103>.
4. Hitchcock SA. Blood-brain barrier permeability considerations for CNS-targeted compound library design. *Curr Opin Chem Biol*. 2008;12:318–23. <https://doi.org/10.1016/j.cbpa.2008.03.019>.
5. Gabathuler R. Approaches to transport therapeutic drugs across the blood-brain barrier to treat brain diseases. *Neurobiol Dis*. 2010;37:48–57. <https://doi.org/10.1016/j.nbd.2009.07.028>.
6. Nau R, Sorgel F, Eiffert H. Penetration of drugs through the blood-cerebrospinal fluid/blood-brain barrier for treatment of central nervous system infections. *Clin Microbiol Rev*. 2010;23:858–83. <https://doi.org/10.1128/CMR.00007-10>.
7. Banks WA. Characteristics of compounds that cross the blood-brain barrier. *BMC Neurol*. 2009;9:S3. <https://doi.org/10.1186/1471-2377-9-S1-S3>.
8. Pajouhesh H, Lenz GR. Medicinal chemical properties of successful central nervous system drugs. *J Am Soc Exp Neurother*. 2005;2:541–53. <https://doi.org/10.1602/neurorx.2.4.541>.
9. Schinkel AH, Wagenaar E, Mol CAAM, Van Deemter L. P-glycoprotein in the blood-brain barrier of mice influences the brain penetration and pharmacological activity of many drugs. *J Clin Invest*. 1996;97:2517–24. <https://doi.org/10.1172/JCI118699>.
10. Nielsen PA, Andersson O, Hansen SH, Simonsen KB, Andersson G. Models for predicting blood-brain barrier permeation. *Drug Discov Today*. 2011;16:472–5. <https://doi.org/10.1016/j.drudis.2011.04.004>.
11. Mensch J, L LJ, Sanderson W, Melis A, Mackie C, Verreck G, et al. Application of PAMPA-models to predict BBB permeability including efflux ratio, plasma protein binding and physicochemical parameters. *Int J Pharm*. 2010;395:182–97. <https://doi.org/10.1016/j.ijpharm.2010.05.037>.
12. Di L, Kerns EH, Fan K, McConnell OJ, Carter GT. High throughput artificial membrane permeability assay for blood-brain barrier. *Eur J Med Chem*. 2003;38:223–32.
13. Syvänen S, Lindhe Ö, Palner M, Lindhe O, Komum BR, Rahman O, et al. Species differences in blood-brain barrier transport of three PET radioligands with emphasis on P-glycoprotein transport. *Drug Metab Dispos*. 2008;37:635–43. <https://doi.org/10.1124/dmd.108.024745>.
14. Lundquist S, Renftel M, Brillault J, Fenart L, Cecchelli R, Dehouck MP. Prediction of drug transport through the blood-brain barrier in vivo: a comparison between two in vitro cell models. *Pharm Res*. 2002;19:976–81.
15. Roux F, Couraud P-O. Rat brain endothelial cell lines for the study of blood-brain barrier permeability and transport functions. *Cell Mol Neurobiol*. 2005;25:41–58. <https://doi.org/10.1007/s10571-004-1376-9>.
16. Andersson O, Hansen SH, Hellman K, Olsen LR, Andersson G, Badolo L, et al. The grasshopper: a novel model for assessing vertebrate brain uptake. *J Pharmacol Exp Ther*. 2013;346:211–8. <https://doi.org/10.1124/jpet.113.205476>.
17. DeSalvo MK, Mayer N, Mayer F, Bainton RJ. Physiologic and anatomic characterization of the brain surface glia barrier of drosophila. *Glia*. 2011;59:1322–40. <https://doi.org/10.1002/glia.21147>. **PHYSIOLOGIC**.
18. Howe K, Clark MD, Torroja CF, Torrance J, Berthelot C, Muffato M, et al. The zebrafish reference genome sequence and its relationship to the human genome. *Nature*. 2013;496:498–503. <https://doi.org/10.1038/nature12111>.
19. Barros TP, Alderton WK, Reynolds HM, Roach AG, Berghmans S. Zebrafish: an emerging technology for in vivo pharmacological assessment to identify potential safety liabilities in early drug discovery. *Br J Pharmacol*. 2008;154:1400–13. <https://doi.org/10.1038/bjp.2008.249>.
20. Fleming A, Diekmann H, Goldsmith P. Functional characterisation of the maturation of the blood-brain barrier in larval zebrafish. *PLoS One*. 2013;8:1–12. <https://doi.org/10.1371/journal.pone.0077548>.
21. Escher BI, Ashauer R, Dyer S, Hermens JLM, Lee JH, Leslie HA, et al. Crucial role of mechanisms and modes of toxic action for understanding tissue residue toxicity and internal effect concentrations of organic chemicals. *Integr Environ Assess Manag*. 2011;7:28–49. <https://doi.org/10.1002/ieam.100>.
22. Tufi S, Leonards P, Lamoree M, De Boer J, Legler J, Legradi J. Changes in neurotransmitter profiles during early zebrafish (*Danio rerio*) development and after pesticide exposure. *Environ Sci Technol*. 2016;50:3222–30. <https://doi.org/10.1021/acs.est.5b05665>.
23. Berghmans S, Butler P, Goldsmith P, Waldron G, Gardner I, Golder Z, et al. Zebrafish based assays for the assessment of cardiac, visual and gut function—potential safety screens for early drug discovery. *J Pharmacol Toxicol Methods*. 2008;58:59–68. <https://doi.org/10.1016/j.vascn.2008.05.130>.
24. Beker van Woudenberg A, Snel C, Rijkmans E, De Groot D, Bouma M, Hermesen S, et al. Zebrafish embryotoxicity test for developmental (neuro)toxicity: demo case of an integrated screening approach system using anti-epileptic drugs. *Reprod Toxicol*. 2014;49:101–16. <https://doi.org/10.1016/j.reprotox.2014.07.082>.
25. Jones HS, Trollope HT, Hutchinson TH, Panter GH, Chipman JK. Metabolism of ibuprofen in zebrafish larvae. *Xenobiotica*. 2012;42:1069–75. <https://doi.org/10.3109/00498254.2012.684410>.
26. Kirla KT, Groh KJ, Steuer AE, Poetzsch M, Banote RK, Stadnicka-Michalak J, et al. Zebrafish larvae are insensitive to stimulation by cocaine: importance of exposure route and toxicokinetics. *Toxicol Sci*. 2016;154:183–93. <https://doi.org/10.1093/toxsci/kfw156>.
27. Chen F, Gong Z, Kelly BC. Rapid analysis of pharmaceuticals and personal care products in fish plasma micro-aliquots using liquid chromatography tandem mass spectrometry. *J Chromatogr A*. 2015;1383:104–11. <https://doi.org/10.1016/j.chroma.2015.01.033>.
28. Kühnert A, Vogs C, Altenburger R, Küster E. The internal concentration of organic substances in fish embryos—a toxicokinetic approach. *Environ Toxicol Chem*. 2013;32:1819–27. <https://doi.org/10.1002/etc.2239>.
29. Brox S, Ritter AP, Küster E, Reemtsma T. A quantitative HPLC-MS/MS method for studying internal concentrations and toxicokinetics of 34 polar analytes in zebrafish (*Danio rerio*) embryos. *Anal Bioanal Chem*. 2014;406:4831–40. <https://doi.org/10.1007/s00216-014-7929-y>.
30. Kantae V, Krekels E, Ordas A, González O, van Wijk RC, Harms AC, et al. Pharmacokinetic modeling of paracetamol uptake and clearance in zebrafish larvae: expanding the allometric scale in vertebrates with five orders of magnitude. *Zebrafish*. 2016;13:504–10. <https://doi.org/10.1089/zeb.2016.1313>.
31. Kalueff AV, Stewart AM, Gerlai R, Court P. Zebrafish as an emerging model for studying complex brain disorders. *Trends Pharmacol Sci*. 2014;35:63–75. <https://doi.org/10.1016/j.tips.2013.12.002>. **Zebrafish**.
32. Jeong JY, Kwon HB, Ahn JC, Kang D, Kwon SH, Park JA, et al. Functional and developmental analysis of the blood-brain barrier in zebrafish. *Brain Res Bull*. 2008;75:619–28. <https://doi.org/10.1016/j.brainresbull.2007.10.043>.
33. Zhuo H, Jin H, Peng H, Huang H. Distribution, pharmacokinetics and primary metabolism model of tramadol in zebrafish. *Mol Med Rep*. 2016;14:5644–52. <https://doi.org/10.3892/mmr.2016.5956>.
34. Kim SS, Im SH, Yang JY, Lee Y-R, Kim GR, Chae JS, et al. Zebrafish as a screening model for testing the permeability of blood-brain barrier to small molecules. *Zebrafish*. 2017;14:322–30. <https://doi.org/10.1089/zeb.2016.1392>.
35. Kulkarni P, Chaudhari GH, Sripram V, Banote RK, Kirla KT, Sultana R, et al. Oral dosing in adult zebrafish: proof-of-concept

- using pharmacokinetics and pharmacological evaluation of carbamazepine. *Pharmacol Rep.* 2014;66:179–83. <https://doi.org/10.1016/j.pharep.2013.06.012>.
36. Hrdina PD, Dubas TC. Brain distribution and kinetics of desipramine in the rat. *Can J Physiol Pharmacol.* 1980;59:163–7.
 37. Bicker J, Alves G, Fortuna A, Falcao A. Blood-brain barrier models and their relevance for a successful development of CNS drug delivery systems: a review. *Eur J Pharm Biopharm.* 2014;87:409–32. <https://doi.org/10.1016/j.ejpb.2014.03.012>.
 38. Benya TJ, Wagner JG. Rapid equilibration of warfarin between rat tissue and plasma. *J Pharmacokinet Biopharm.* 1975;3:237–255.
 39. DeVane CL, Boulton DW, Miller LF, Miller RL. Pharmacokinetics of trazodone and its major metabolite m-chlorophenylpiperazine in plasma and brain of rats. *Int J Neuropsychopharmacol.* 1999;2:17–23. <https://doi.org/10.1017/S1461145799001303>.
 40. O'Byrne PM, Williams R, Walsh JJ, Gilmer JF. Part two: evaluation of N-methylbupropion as a potential bupropion prodrug. *Pharmaceuticals.* 2014;7:676–94. <https://doi.org/10.3390/ph7060676>.
 41. Hendrickx S, Uğur DY, Yilmaz IT, Şener E, Van Schepdael A, Adams E, et al. A sensitive capillary LC-UV method for the simultaneous analysis of olanzapine, chlorpromazine and their FMO-mediated N-oxidation products in brain microdialysates. *Talanta.* 2017;162:268–77. <https://doi.org/10.1016/j.talanta.2016.09.053>.
 42. Kislyuk S, Kroonen J, Adams E, Augustijns P, De Witte P, Cabooter D. Development of a sensitive and quantitative UHPLC-MS/MS method to study the whole-body uptake of pharmaceuticals in zebrafish. *Talanta.* 2017;174:780–8. <https://doi.org/10.1016/j.talanta.2017.06.075>.
 43. EMA. Guideline on bioanalytical method validation. EMEA, Comm Med Prod Hum Use. 2012;44:1–23.
 44. Lee M, Hong S, Kim N, Shin KS, Kang SJ. Tricyclic antidepressants amitriptyline and desipramine induced neurotoxicity associated with Parkinson's disease. *Mol Cells.* 2015;38:734–40. <https://doi.org/10.14348/molcells.2015.0131>.